The pH and Substrate Effect on Adsorption of Peptides Containing Z and E Dehydrophenylalanine. Surface-Enhanced Raman Spectroscopy Studies on Ag Nanocolloids and Electrodes.

ARTICLE *in* THE JOURNAL OF PHYSICAL CHEMISTRY B · MARCH 2014

Impact Factor: 3.3 · DOI: 10.1021/jp500650p · Source: PubMed

3 AUTHORS, INCLUDING:

Kamilla Malek
Jagiellonian University
47 PUBLICATIONS **226** CITATIONS

SEE PROFILE

THE JOURNAL OF PHYSICAL CHEMISTRY B

Article

pubs.acs.org/JPCB

pH and Substrate Effect on Adsorption of Peptides Containing *Z* and *E* Dehydrophenylalanine. Surface-Enhanced Raman Spectroscopy Studies on Ag Nanocolloids and Electrodes

Kamilla Malek,*[,†] Agata Królikowska,[‡] and Jolanta Bukowska[‡]

[†]Faculty of Chemistry, Jagiellonian University, Ingardena 3, 30-060 Krakow, Poland

[‡]Faculty of Chemistry, University of Warsaw, Pasteura 1, 02-093 Warsaw, Poland

Supporting Information

ABSTRACT: The silver substrates and pH dependent surface-enhanced Raman scattering (SERS) spectra of unsaturated derivatives of di- and tripeptides (dehydropeptides) are investigated. Experimental spectra were interpreted with the help of DFT calculations and normal-mode analysis. We choose as objects of our studies modified but natural peptides containing *Z* or *E* dehydrophenylalanine ($^{(Z)/(E)}\Delta$Phe) residue to study an effect of the type of the isomer on the interaction between the peptide and silver surfaces in the form of nanocolloidal particles and an electrochemically roughened electrode. We also observed that the SERS profile is sensitive to both the type of the studied SERS active substrate and pH, especially for the adsorption on the silver colloid. In general, all dehydropeptides interact with both SERS substrates upon deprotonation of the C-end of the molecule. The participation of the other fragments of the adsorbates such as the N-terminal amino group and the dehydroresidue is also manifested in the SERS spectra. Their orientation with respect to the silver surfaces is discussed in detail.

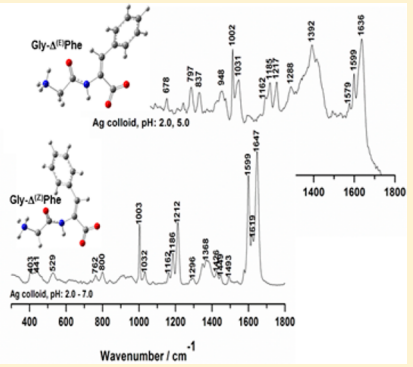

1. INTRODUCTION

Normal Raman and surface-enhanced Raman spectroscopy is a powerful tool in the characterization of biologically active species such as proteins, nucleic acids, drugs, etc.[1] Both techniques are sensitive to the even slight changes in the molecular structure, as well as the chemical environment. SERS refers to the extraordinarily large enhancement of Raman signals that are obtained from roughened surfaces or aggregated small nanoparticles of certain metals, usually silver, gold, and copper. The most used SERS substrates are metal electrodes and colloidal nanoparticles because of their low costs as well as a simple manipulation. Obviously, roughness of a SERS substrate affects the adsorption mechanism of a molecule by changing strength of the metal−adsorbate interactions and/or an adsorption site. Despite this, Coulombic stabilization between the metal surface and the adsorbate is required to observe surface-enhanced Raman scattering; thus when the electrode surface or colloidal particles and the analyte have charges of the same sign, the adsorption process can be strongly hindered. Consequently, an orientation of the adsorbate on the metal as well as detection level of an analyte can be completely different, when various metal substrates are used in SERS experiment.[1] Hence, the investigation of the substrate influence, its interfacial properties, and molecular specificity is crucial for a better understanding of the SERS enhancement for a given molecule. The Raman profile of amino acids, peptides, and proteins, especially those adsorbed on the metal surface investigated in SERS experiment, has been widely studied by several groups.[2−7] Because of the large Raman cross-section of the aromatic moieties, SERS spectra of aromatic peptides or proteins are dominated by bands assigned to vibrations of the phenyl ring. The latter is accompanied by the bands of the deprotonated C-terminal end of a biomolecule and rarely by modes of the amino groups or the peptide backbone.

In turn, introducing α,β-dehydrophenylalanine (ΔPhe) residue into the backbone of a peptide sequence affects both chemical reactivity and conformation, because this residue contains a double C−C bond between the α and β carbon atoms. The presence of this bond decreases the conformational flexibility of proteins. Additionally, the ΔPhe moiety exists in the two isomeric forms, *Z* and *E*, which can influence the biological activity of the peptide.[8] This class of nonproteinogenic amino acids can be found in many biological peptides with antiviral, antitumor, anti-inflammatory, or immunosuppressive activities.[9,10] Dehydroamino acids are also used in de novo synthesis of protein mimics for structure−function relationship studies.[11,12] In addition, potentiometric and electronic absorption studies on coordination ability of dehydropeptides toward Ni(II) and Cu(II) ions have shown that the presence of the double $C_\alpha C_\beta$ bond makes the dehydropeptides more efficient ligands than the parent peptides.[13,14] These dehydropeptides form various coordina-

Received: January 20, 2014
Revised: March 13, 2014

   dx.doi.org/10.1021/jp500650p | *J. Phys. Chem. B* XXXX, XXX, XXX−XXX

tion modes, in which N atoms of the N-terminal amino group and of amide bonds are usually metal binding sites. In addition, ligands with the phenyl ring in the *Z* configuration show distinctly higher ability of metal ion binding through nitrogen atoms, when compared to peptides with $\Delta^{(E)}$Phe.[13,14] The deprotonated carboxylic group also participates in coordination of the metal ions, but this interaction is much weaker for the *Z* isomer of ΔPhe than the *E* counterpart due to the steric hindrance. This effect was observed to be stronger for short peptides.[13,14] Recently, several experimental and theoretical studies on molecular structure of dehydropeptides have been reported, but they have been focused mainly on the analysis of IR,[8,15] circular dichroism,[16] NMR spectra,[15] and X-ray diffraction[15−17] supported by quantum-chemical calculations.[18,19] Up to now, the Raman and SERS profiles of short peptides containing dehydroamino acid residues have been studied by our group only.[20,21] In our previous work[20] we reported IR, Raman, and SERS spectra of three dipeptides Boc-Gly-X, where X is ΔAla, $\Delta^{(Z)}$Phe, and $\Delta^{(E)}$Phe. SERS spectra were collected by using Ag sol as a metal substrate. Here, the dehydropeptide−metal interactions occur mainly due to deprotonation of the terminal carboxylic group. The adsorption process strongly affects the appearance of SERS bands in the region 1500−1650 cm^{-1}, indicating possibility of π-electron resonance between the phenyl ring and the peptide backbone. Thus, to continue these investigations, we study in this work adsorption mechanism of di- and tripeptides containing $\Delta^{(Z)}$Phe and $\Delta^{(E)}$Phe residues, i.e., Gly-$\Delta^{(Z)}$Phe (^{Z}diP), Gly-$\Delta^{(E)}$Phe (^{E}diP), Gly-$\Delta^{(Z)}$Phe-Gly (^{Z}triP), and Gly-$\Delta^{(E)}$Phe-Gly (^{E}triP) by means of surface-enhanced Raman spectroscopy. The structures of the peptides are depicted in Figure 1. IR and

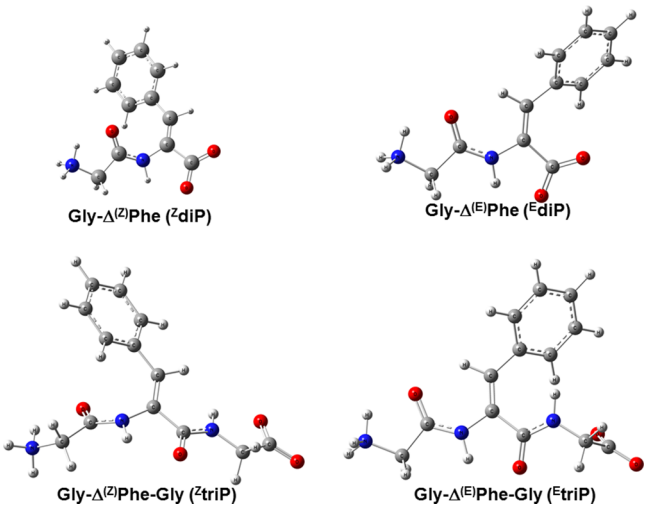

Figure 1. Optimized structures of the dehydropeptides computed by using PCM/B3LYP/6-311++G(d,p).

Raman spectra were also recorded and analyzed to give an unequivocal assignment of fundamental modes, with a support of DFT calculations. Next, we recorded surface-enhanced Raman spectra on the silver substrates (colloid and electrode) by using a VIS excitation line. The SERS studies were performed to determine the nature of the interaction of these peptides with different silver surfaces as well as to determine how the type of the isomer and the number of amino acid residues affect peptide ability to adsorb on the silver surfaces. Because the studied molecules exist as zwitterions, we also investigate their adsorption behavior due to pH changes in the range 2−9. Their protonation constants in aqueous solution slightly differ, and they were determined in the ranges 2.34−3.41 and 7.82−8.09 for the carboxylic and amino groups, respectively.[13,14] Therefore, in our experiment the peptides should exist in solution as $^{+}H_3N$-R-COOH, $^{+}H_3N$-R-COO^{-}, and H_2N-R-COO^{-} species at pHs of 2.0, 5.0/7.0, and 9.0, respectively. The presence of the various de/protonated states can lead to several adsorption modes and/or preferable conformations that can easily interact with the metal surface. In the case of the peptides studied here the most possible site of the interaction with the metal is the deprotonated C-terminal carboxylic group and the phenyl ring, on the contrary to the NH_3^{+} group.[20] However, one should keep in mind that the adsorption process on the SERS-active substrates cannot be solely evaluated from the pK_a values of deprotonation of the amino and carboxylic groups in solution, because acid−base properties can change upon adsorption on a metal surface.[1]

2. EXPERIMENTAL METHODS

2.1. Preparation of Samples. Dehydropeptides were synthesized according to procedures described previously.[14,20,22] Stock solutions of 0.1 M concentrations were prepared in 4-fold distilled water. The pH of the analyte solutions (2.0, 5.0, 7.0, and 9.0) was adjusted by adding 0.01 M HCl or NaOH. All the reagents employed were of analytical grade and purchased from Aldrich-Sigma.

2.2. Preparation of Silver Substrates and Samples for SERS Measurements. The silver colloid was prepared following the Lee and Meisel procedure by adding silver nitrate to an aqueous solution of sodium citrate as a reducing agent.[23] The UV−vis spectra of colloids were recorded on an Evolution 60 spectrophotometer with a resolution of 1 nm in a region of 190−1100 nm in a quartz cell of 1 cm. Two batches of colloids were prepared, and their resonant absorption bands appeared in the range 415−428 nm. To prepare a sample for SERS measurements, 20 μL of 10 mM analyte solution was added to 1 mL of the colloid, after activation of the colloid by 40 μL of 0.5 M KNO_3 or KCl. Hence, the final concentration of the analyte was around 10^{-4} M.

The silver electrodes were prepared by electrochemical roughening, using five positive/negative cycles in 0.1 M KCl solution from −0.3 to +0.3 V (vs Ag/AgCl) and the potential close to the end of the last negative cycle was held for 30 s. A platinum electrode was used as a counter electrode and Ag/AgCl in 1 M KCl was used as a reference. The Ag electrodes were immersed in 10 mM aqueous solutions of the peptides. For both Ag substrates, we recorded SERS spectra for solutions with a concentration in the range 10−0.01 mM. However, stable enhancement of the intensity of Raman bands was observed only for 0.1 and 10 mM for the colloid and electrode surface, respectively. The overall spectral pattern remained unchanged, independent of the concentration. Use of relatively high concentration in solution, particularly for the metal electrodes was imposed by the fragility of the of adsorbate films to thermal decomposition, induced by enhanced electric field.

2.3. Instrumentation. The FT-IR ATR (375−4000 cm^{-1}) spectra of the solid compounds (ca. a few mg of a sample placed on the surface of a diamond ATR crystal with 0.5 mm diameter) were recorded using a Bruker Alpha spectrometer, fitted with a deuterated L-alanine doped triglycine sulfate (DLATGS) detector. A total of 128 scans, with a spectral resolution of 4 cm^{-1}, were accumulated. For FT-Raman

dx.doi.org/10.1021/jp500650p | J. Phys. Chem. B XXXX, XXX, XXX−XXX

measurements, a few milligrams of the solid dehydropeptides and their 0.1 M solutions was directly measured on metal discs and in glass cuvettes, respectively, and 512 and 1600 scans were collected (with a resolution of 4 cm^{-1}) for the solid and solution samples, respectively. Spectra were recorded on a FT-Raman spectrometer Bruker Ramanscope III equipped with a Nd:YAG laser, emitting at 1064 nm, and a germanium detector, cooled with liquid nitrogen. The output power of the laser was 50 and 350 mW for solids and solutions, respectively.

SERS spectra of the peptides on the Ag substrates were collected in the backscattering configuration with a Labram HR800 (Horiba Jobin Yvon) confocal microscope system, equipped with a Peltier-cooled CCD detector (1024 × 256 pixel), using a HeNe laser (632.8 nm). The output laser power (on the head) was 20 mW. The confocal pinhole size was set to 200 μm and the holographic grating with 600 grooves/mm was used. The calibration of the instrument was performed using a 520 cm^{-1} Raman signal of a silicon wafer. For colloidal solution measurements a cuvette holder and 1 cm quartz cuvette were used. For each SERS spectrum 4 scans were collected with integration times of 10−15 s. The SERS spectra on the Ag electrode were obtained using a 50× magnification Olympus objective and accumulated 1−5 scans, ranging from 3 to 20 s.

2.4. Modeling of Vibrational Spectra. Computational Details. To assign the observed IR, Raman, and SERS bands, normal vibrational modes, IR intensity, and Raman activity were computed and then correlated with experimental IR and Raman spectra. All calculations were performed with the Gaussian 09 program for the purpose of modeling IR and Raman spectra with the PED assignment of the bands.[24] The ground state geometries of dehydropeptides were investigated using the Kohn−Sham density functional theory (DFT). The DFT with Becke's three-parameter (B3),[25] combined with the Lee−Yang−Parr (LYP) gradient-corrected functional (B3LYP)[26] were employed with the 6-311++G(d,p) basis set. The optimization process and calculations of harmonic wavenumbers were performed using Tomasi and co-workers'[27] polarizable continuum model (PCM) for water. This method was applied to perform calculations for zwitterion forms of the peptides studied here; otherwise the optimization process starting from the zwitterionic model led to the proton transfer from the NH_3^+ group to the COO^- moiety. Such an approach has been widely used in calculations of molecular structure and vibrational spectra of amino acids and short peptides, as reported in the literature.[28,29]

No imaginary frequencies were obtained, which indicate that the optimized molecular structures correspond to minima on the potential energy surface. The computed harmonic wavenumbers, IR intensities, and Raman scattering activities were used in the further modeling of IR and Raman spectra. To accomplish it, theoretical Raman intensities (I_i^R) were obtained from the Gaussian 09 calculated Raman scattering activities (S_i) for solids, according to the expression $I_i^R = 10^{-12}(\nu_0 - \nu_i)^4 \nu_i^{-1} S_i$, where ν_0 is the frequency of the laser excitation line and ν_i is the frequency of normal mode i.[30] Prior to the comparison of the calculated wavenumbers with their experimental counterparts (IR and Raman spectra), the wavenumbers were scaled down by appropriate scaling factors (0.978 and 0.960 for the 0−2000 and 2000−4000 cm^{-1} regions, respectively) mainly to account for anharmonicity effects, basis set truncation, and the neglected part of electron correlation. These scaling factors have been successfully used by our group in calculations of IR and Raman spectra of numerous organic compounds.[20,31,32] In addition, to provide an unequivocal assignment of the calculated IR and Raman modes, normal coordinates analysis calculations were performed using a set of internal coordinates defined as suggested by Pulay and Fogarasi.[33,34] The GAR2PED program was used for the calculation of potential energy distribution (PED) of normal modes in terms of natural, internal coordinates.[33] Definitions of the internal coordinates used in this work are collected in Table 1S (Supporting Information).

3. RESULTS AND DISCUSSION

3.1. IR and Raman Profile of the Dehydropeptides in the Solid State and Solutions. The FT-IR spectra of the solid samples are presented in Figure 2 and the comparison of normal FT-Raman spectra of the solids and the solutions is shown in Figures 3A−6A. The selected bands positions of the FT-IR and FT-Raman spectra of the solid samples together with the assignment of the vibrational modes are collected in Tables 1−4. The underlying aim of recording both the FT-IR and FT-Raman spectra, additionally to the SERS signal, is to apprehend the existence of the preferential form of the molecules in the solid state/solution and on the metal substrate after assignment of the vibrational signatures. The optimized structures of the peptides are shown in Figure 1, and the comparison of experimental IR and Raman spectra in the solid state with the computed ones is presented in Figures 1S−4S (Supporting Information). Here, we present an overall discussion to point out similarities and differences in the experimental spectral profile of the studied compounds in the

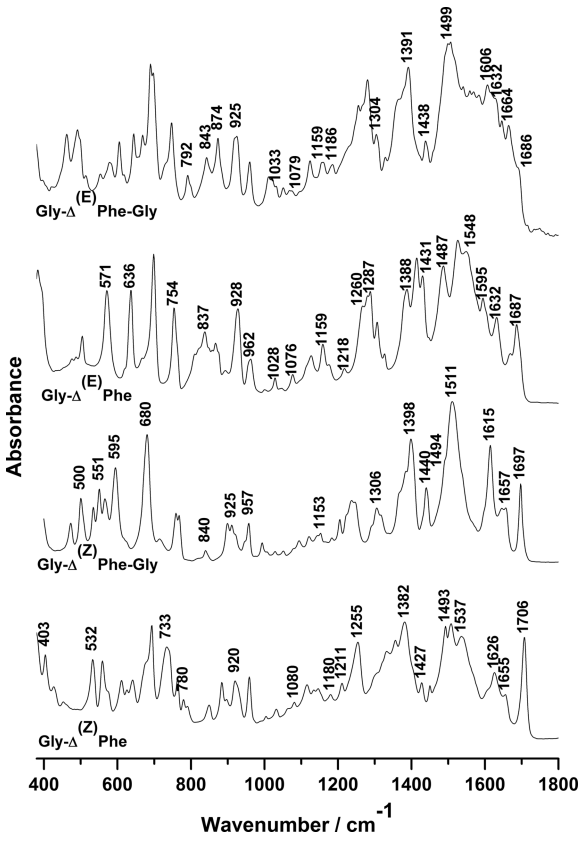

Figure 2. FT-IR ATR spectra of the solid dehydropeptides studied here in the spectral region 400−1800 cm^{-1}.

dx.doi.org/10.1021/jp500650p | J. Phys. Chem. B XXXX, XXX, XXX−XXX

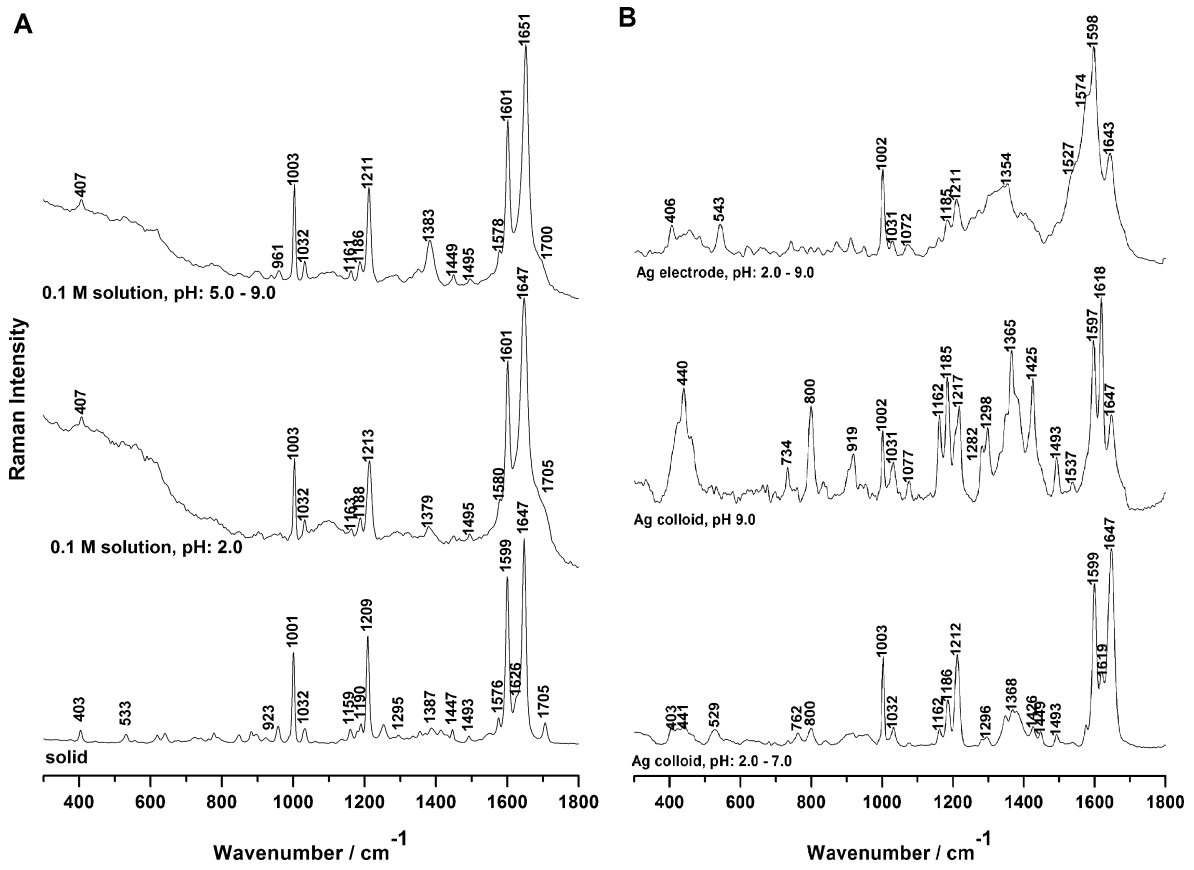

Figure 3. FT-Raman spectra of the solid state and the aqueous solutions (1064 nm) (A) and SERS spectra (633 nm) on the Ag colloid and electrode (B) of Gly-$\Delta^{(Z)}$Phe in the spectral range 300−1800 cm^{-1}.

region 400−1800 cm^{-1} that is necessary for the further analysis of the SERS results.

Because IR spectra of aqueous solutions are dominated by water vibrations, we cannot discuss them in terms of pH changes. The IR profiles of the four dehydropeptides differ in the studied region (Figure 2), indicating a strong influence of the type of isomer as well as the number of amino acid residues on molecular structure. The region within 1500−1700 cm^{-1}, which is sensitive to the peptide secondary structure, exhibits many overlapping bands. They mainly originate from amide I/II vibrations, the C═C stretching mode, phenyl ring vibrations, and the asymmetric modes of the terminal groups, i.e., NH_3^+ and COO^- (Tables 1−4). The comparison of the spectra of the dipeptides indicates that amide I vibration is significantly red-shifted by ca. 20 cm^{-1} for the *E* isomer in comparison to the *Z* counterpart (cf. Tables 1 and 2) and both the bands appear at relatively high wavenumber, above 1680 cm^{-1}. In turn, the bending NH mode contributing to the amide II mode of dipeptides is observed at 1508/1537 and 1548 cm^{-1} for ^{Z}diP and ^{E}diP, respectively. This suggests that the molecules of ^{E}diP are involved in stronger H-bonding than the *Z* isomer.[34] Interestingly, we observed in our previous work[20] that the amide I mode in Boc-Gly-ΔPhe appears at 1672 and 1627 cm^{-1} in the IR spectra of the *Z* and *E* isomers, respectively. This suggests that the introduction of the bulk *tert*-butoxycabonyl group into the backbone of the peptides causes a shift of the amide I mode by 30−50 cm^{-1}.

DFT computations indicated that amide I vibrations of both peptide bonds of the tripeptides should be attributed to separate bands, i.e., the amide I mode of the Gly-ΔPhe- moiety to a band at a higher wavenumber than for the -ΔPhe-Gly fragment. However, the presence of the two closely located amide moieties within the tripeptide molecule results in a very likely intramolecular coupling of their vibrational modes. Therefore, we propose to assign the IR and Raman bands of both tripeptides in the region 1630−1700 cm^{-1}, arising respectively at a lower and higher wavenumber, to the in- and out-of-phase coupled amide I vibrations of both peptide units (Tables 3 and 4). The fact that the former is stronger in Raman and the latter is stronger in the IR spectrum of the solid peptides supports this assignment. Both amide I bands of ^{E}triP are shifted toward lower wavenumbers by 30−50 cm^{-1} in comparison to ^{Z}triP, indicating the presence of strong intermolecular H-bonding for the *E* isomer, similarly to the dipeptides. In turn, IR bands at ca. 1540 and 1510 cm^{-1} are assigned to the amide II mode. The correlation between the secondary structure and positions of amide modes in IR spectra has been previously discussed for a series of N- and C-blocked dehydropeptides.[21] Accordingly, IR spectra of Boc-Gly-$\Delta^{(Z)}$Phe-Gly-OMe and Boc-Gly-$\Delta^{(E)}$Phe-Gly-OMe exhibit the presence of amide I bands attributed to α-helical (ca. 1660, 1685 cm^{-1}) as well as β-turn (ca. 1620−1640, 1690−1720 cm^{-1}) conformations whereas bands of the amide II mode are observed at ca. 1510 and 1540 cm^{-1} for both tripeptides. This indicates that the positions of amide modes for ^{Z}triP and ^{E}triP are found in the spectral region typical for α-helical and folded structures, respectively.

Figures 3A−6A show the normal FT-Raman spectra of solid dehydropeptides compared to spectra of aqueous solutions at various pH. The Raman signature of proteins containing

dx.doi.org/10.1021/jp500650p | J. Phys. Chem. B XXXX, XXX, XXX−XXX

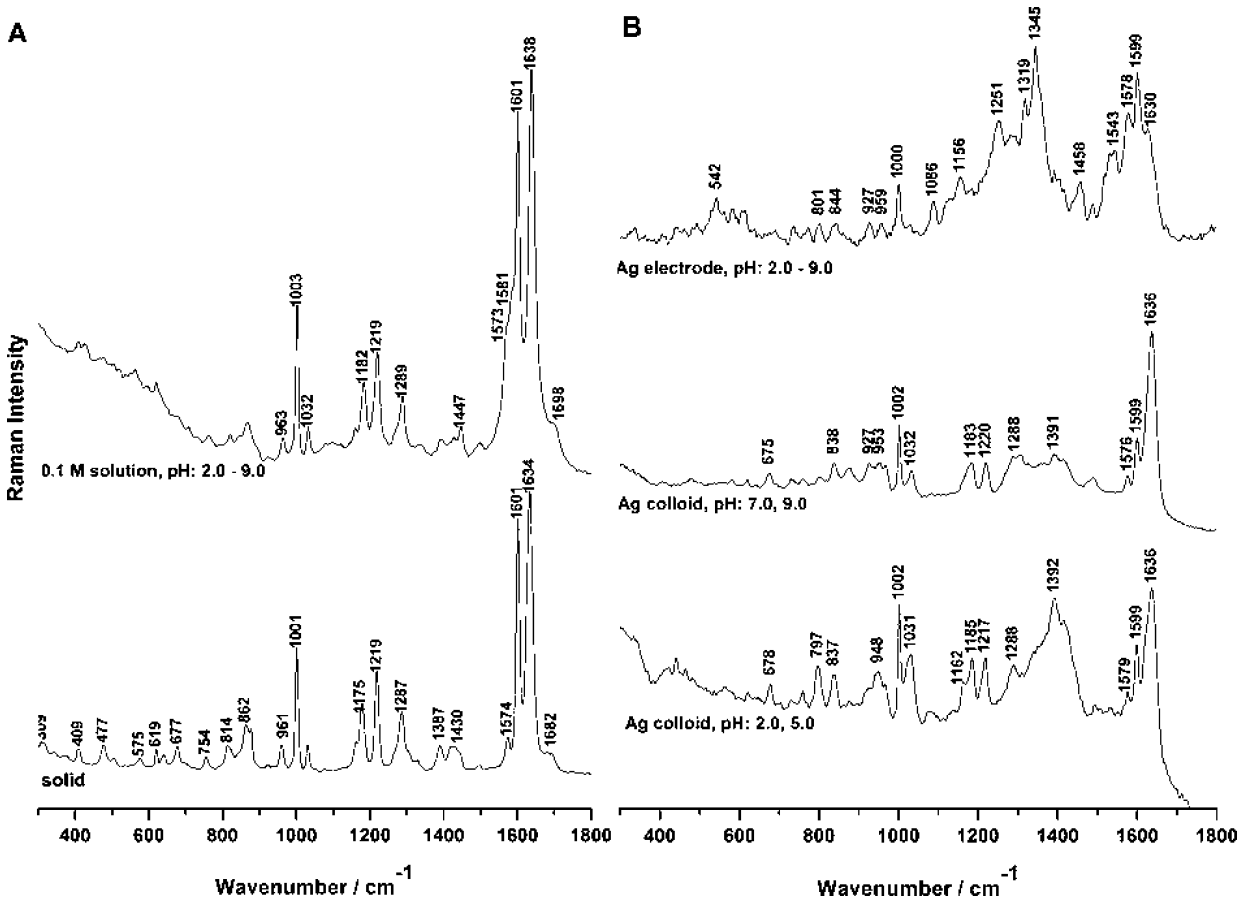

Figure 4. FT-Raman spectra of the solid state and the aqueous solutions (1064 nm) (A) and SERS spectra (633 nm) on the Ag colloid and electrode (B) of Gly-$\Delta^{(E)}$Phe in the spectral range 300−1800 cm^{-1}.

aromatic amino acids is dominated by the fundamental modes involving the aromatic side chain and peptide backbone (Tables 1−4). Among the vibrations of the phenyl ring, the symmetric breathing mode 12 at ca. 1000 cm^{-1}, the ring CC stretching 8a vibration at ca. 1600 cm^{-1}, the 13 mode involving the C_β—C_{Ph} stretching mode at ca. 1205−1220 cm^{-1} are the most intense Raman bands. In contrast to the 12 and 8a modes that are insensitive to the nature of substituents, the position and intensity of the 13 vibration of the phenyl ring are affected by the type of the peptides isomer studied here. This mode includes the stretching motion of the C_β—C_{Ph} bond. High-intensity Raman bands assigned to this vibration are observed at 1209 and 1205 cm^{-1} for ^{Z}diP and ^{Z}triP peptides, respectively, whereas medium-intensity Raman bands around 1220 cm^{-1} are found for the peptides containing the *E* isomer. This indicates shortening of the C_β—C_{Ph} bond for the *E* derivatives. The intensity and positions of these bands are roughly conserved in the spectra of the aqueous solutions. The marker band for the C_α=C_β moiety appears as a very intensive Raman band in the region 1610−1660 cm^{-1} [$\nu(C_\alpha{=}C_\beta)$]. Here, the position of this band is red-shifted by at least 15 cm^{-1} along with the elongation of the peptide backbone. This appears in the region 1630−1650 and 1615−1620 cm^{-1} for di- and tripeptides, respectively, suggesting shortening of the C_α=C_β bond in the tripeptides. Apart from that, no correlation is found for changing the isomer from *Z* to *E*. This band is down-shifted in the spectra of dipeptides on the contrary to the tripeptides. Interestingly, the Raman spectra of the Boc-Gly-ΔPhe peptides show that this mode appears at the same wavenumber, 1648 cm^{-1}, for both isomers.[20] But the N- and C-blocked tripeptides containing $\Delta^{(Z/E)}$Phe exhibit an effect similar to that observed here. The change of the isomer type from *Z* to *E* causes the 9 cm^{-1} shift of $\nu(C_\alpha{=}C_\beta)$ toward higher wavenumbers.[21] This finding suggests that the position of this marker band is sensitive to molecular structure of the dehydropeptide rather than to the isomer type. Depending on the pH values, the peptides studied here can exist in the protonated or deprotonated state in the aqueous solution, as mentioned in the Introduction. However, the normal Raman spectra of the solutions (cf. Figures 3A−6A) show mainly the presence of the bands assigned to vibrations of the phenyl ring and the C_α=C_β bond. The relative intensities and wavenumbers of bands are roughly conserved in comparison to Raman spectra of the solids. Some changes in a spectral profile of aqueous solutions are observed but they cannot be correlated with the transition between the species formed due to the pH change. Only Raman spectra of ^{Z}diP evidence deprotonation of the carboxylic group upon the increase of pH by the appearance of a medium-intensity band at 1383 cm^{-1} [$\nu_s(COO^-)$] (Figure 3A).

3.2. Effect of pH and the Metal Substrate on SERS Spectra of the Dehydropeptides. Tables 1−4 show the main wavenumbers found in all the SERS spectra recorded in this studies along with the assignments deduced from our DFT calculations.

Gly-$\Delta^{(Z)}$Phe (^{Z}diP). Figure 3B shows SERS spectra of the $\Delta^{(Z)}$Phe dipeptide, and positions of SERS bands along with their assignments are collected in Table 1. The SERS features recorded on the Ag colloid in the pH range 2−7 are similar but

dx.doi.org/10.1021/jp500650p | J. Phys. Chem. B XXXX, XXX, XXX−XXX

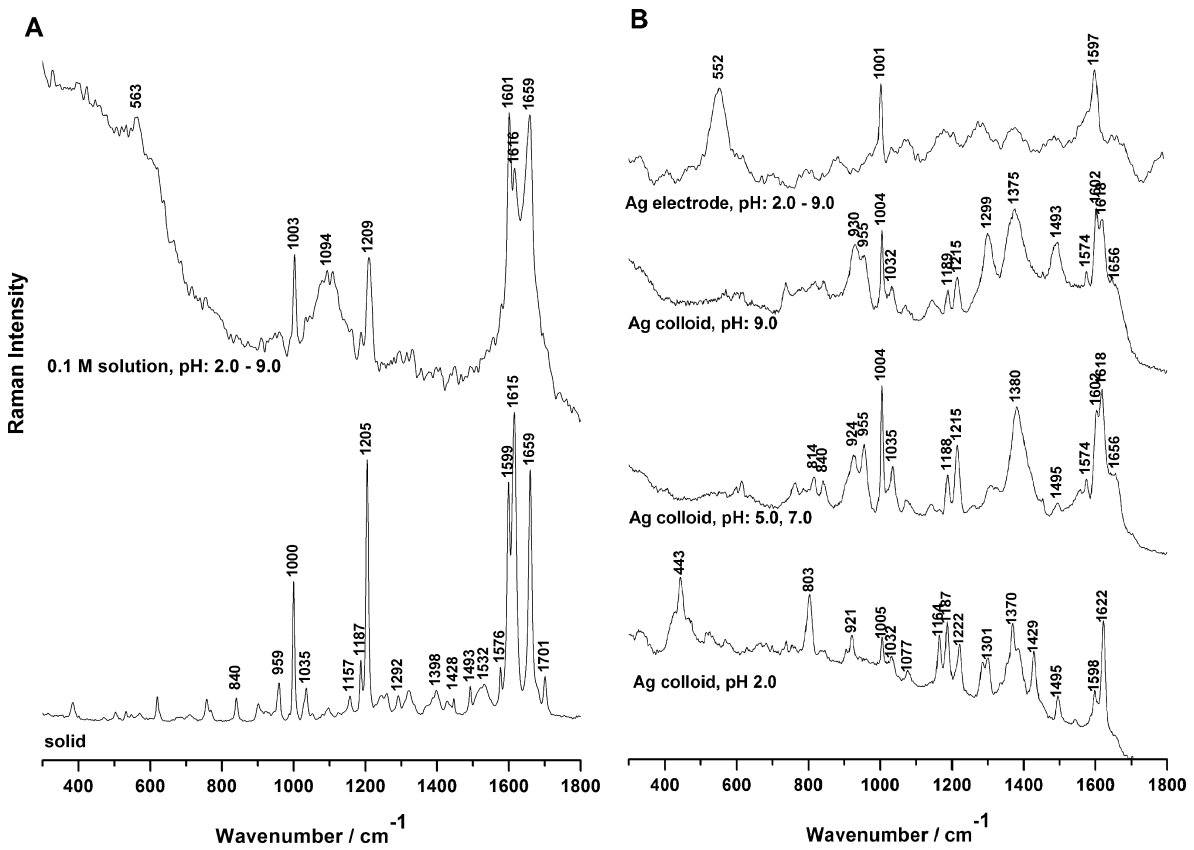

Figure 5. FT-Raman spectra of the solid state and the aqueous solutions (1064 nm) (A) and SERS spectra (633 nm) on the Ag colloid and electrode (B) of Gly-$\Delta^{(Z)}$Phe-Gly in the spectral range 300−1800 cm^{-1}.

completely differ from the alkaline solution (pH 9). Below pH of 7, $^{+}H_3N$-R-COOH/COO^{-} species were introduced to the colloidal solutions, whereas H_2N-R-COO^{-} should exist exclusively at pH 9. In turn, the interaction of ^{Z}diP with the silver electrode is insensitive to the pH of the environment. This SERS spectrum is dissimilar to any SERS spectrum recorded on the metal colloid, thus demonstrating the appearance of another adsorption mechanism on the Ag electrode.

In the spectrum recorded under pH 2−7 in the silver sol, the most intense bands at 1599 and 1647 cm^{-1} are assigned to the 8a and $\nu(C_\alpha{=}C_\beta)$ vibrations, respectively. Their relative intensities and positions do not change due to interaction with the Ag colloidal particles (cf. Figure 3A,B). The other prominent bands, which appear at 1003, 1186, and 1212 cm^{-1}, are attributed to the in-plane modes of the phenyl ring, i.e., 12, 9a, and 13, respectively. According to the SERS selection rules for electromagnetic mechanism,[35] it is likely that the phenyl ring of ^{Z}diP at pH 2−7 adopts a tilted orientation. In turn, SERS bands with maxima at 800 and 1368 cm^{-1} are attributed to the scissoring and symmetric stretching vibrations of the COO^{-} group, respectively. This indicates the appearance of the deprotonated carboxylic group after interaction with the silver sol, even though the molecules were introduced to the colloid mainly as the protonated species (like at pH 2). The loss of the COOH proton upon the adsorption onto the silver nanoparticles is a well-documented fact.[36−38] Moreover, the SERS band at 1368 cm^{-1} at pH 2−7 is very broad and shows a few components that can be explained by slightly different orientations of the carboxylate group on the silver. Because the corresponding band in the normal Raman spectra of the solutions is observed around ca. 1380 cm^{-1}, the red shift of the SERS band by ∼15 cm^{-1} indicates an elongation of the C−O bonds in the COO^{-} group. On the basis of Suh and Kim's report on the geometry of surface-adsorbed carboxylate groups,[36] we propose here that the carboxylate group is almost parallel to the surface and adsorbed through π-electrons, because the $\nu_s(COO^{-})$ band is stronger than $\delta(COO^{-})$ band at 800 cm^{-1}.

Upon an increase of pH to 9, enhancement of all band intensities is observed. However, this enhancement is not the same for all spectral features. The band intensities of the vibrations of both terminal groups, i.e., C-terminus and N-terminus, located at 800, 1365, and 1618 cm^{-1} increase significantly along with appearing new features assigned to vibrations of the end groups at 734, 1077, and 1537 cm^{-1} (Figure 3B and Table 1). The intensity increase of the $\delta(COO^{-})$ mode at 800 cm^{-1} with respect to $\nu_s(COO^{-})$ at 1365 cm^{-1} indicates that the C-end of the peptide adopts here a more tilted orientation than in the less alkaline solution. The most prominent change in this SERS spectrum is a considerable enhancement of the 1618 cm^{-1} band, assigned to the bending vibration of the amino group. The same band is observed at pH 2−7, but only as a weak shoulder at 1619 cm^{-1} in the SERS spectrum in Figure 3B. At first glance, this band could be attributed, according to DFT calculations, to the asymmetric scissoring mode of the terminal protonated amino group ($\delta_{as}(NH_3^{+})$) that is found in the NR spectrum of the solid at 1626 cm^{-1}. Under acidic pH this form of the amino group should be dominant in the SERS experiment, supporting the assignment. However, a Raman band at ca. 1614 cm^{-1} can also implicate the bending mode of the NH_2 group as observed in

dx.doi.org/10.1021/jp500650p | J. Phys. Chem. B XXXX, XXX, XXX−XXX

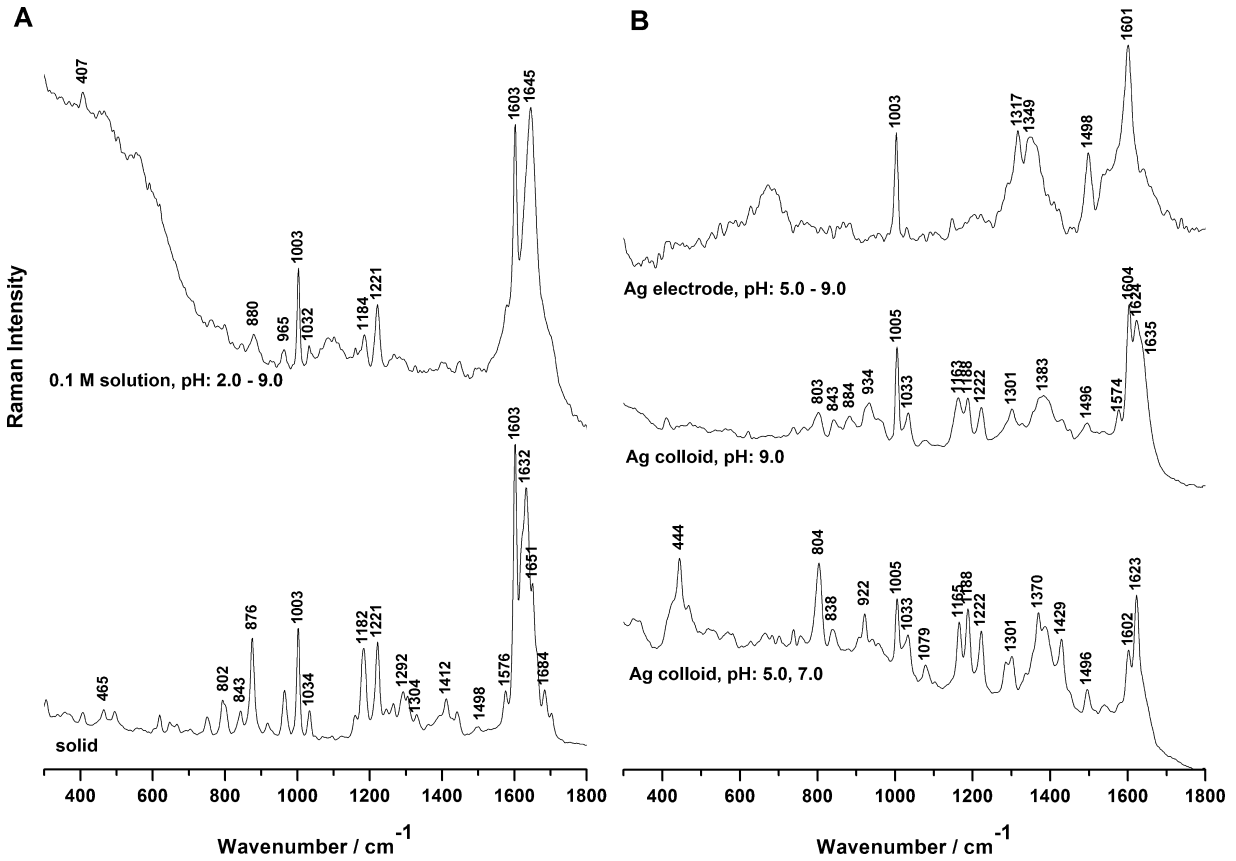

Figure 6. FT-Raman spectra of the solid state and the aqueous solutions (1064 nm) (A) and SERS spectra (633 nm) on the Ag colloid and electrode (B) of Gly-$\Delta^{(E)}$Phe-Gly in the spectral range 300−1800 cm^{-1}.

SERS spectrum of α-phenylglycine,[38] which could indicate deprotonation of the amino group. This interpretation is more relevant for pH 9, as the considerable increase of this band (at 1619 cm^{-1}) intensity is observed upon alkalization.

The other pronounced feature of SERS behavior of ^{Z}diP adsorbed from the alkaline solution is a different enhancement of the vibrational modes of the π-electron rich functional groups. Comparing to the SERS spectrum at pH 2−7, we see that the $\nu(C_\alpha{=}C_\beta)$ intensity (at 1647 cm^{-1}) markedly decreases, whereas the relative intensity of some modes of the phenyl ring alters in a clearly noticeable manner. Namely, bands at 440, 1162, 1185, and 1425 cm^{-1} assigned to the 16b, 9b, 9a, and 19b modes, respectively, are enhanced strongly in comparison with the normal Raman and SERS at pH 2−7 spectra (Figure 3A,B). The relatively large enhancement of the out-of-plane vibration 16b at 440 cm^{-1} likely results from a more flat orientation of the ^{Z}diP phenyl ring with respect to the Ag surface, whereas a peak broadening may suggest a nonuniform orientation of the molecules via the phenyl ring.

The SERS spectrum of ^{Z}diP on the silver electrode obtained by exciting at the same radiation wavelength (632.8 nm) is shown in Figure 3B. This spectrum is dissimilar to that obtained on the silver sol, thus demonstrating another adsorption pattern. Likely, this results from the slightly positive charge of the electrode surface at open circuit potential, in comparison to the negatively charged Ag nanoparticles in the sol (due to the presence of adsorbed citrate anions). All bands observed in the SERS spectrum in Figure 3B are assigned to modes of the benzylidene and COO^- groups only (cf. Table 1). Similarly to the previous SERS experiment, the intensity of a band corresponding to the $\nu(C_\alpha{=}C_\beta)$ vibration is weaker than that of the 8a mode of the phenyl ring at 1598 cm^{-1}, whereas the band of $\delta_{as}(NH_3^+)$ at ca. 1618 cm^{-1} is not observed as it is expected for repulsive forces between the positively charged Ag surface and the amino group. The distinctive feature of this SERS spectrum is a strongly enhanced band at 1574 cm^{-1}, being a shoulder of a 1598 cm^{-1} band. This band appears in the region typical for the asymmetric 8b mode (b_2) of the phenyl ring (DFT, 1576 cm^{-1}; Raman/solid, 1576 cm^{-1}) and the asymmetric stretching vibration of the COO^- group, $\nu_{as}(COO^-)$ (DFT, 1585 cm^{-1}; IR/solid, ca. 1600 cm^{-1}). If this band originates from the 8b mode, the enhancement of the asymmetric vibration may indicate a large contribution of a charge-transfer resonance into the surface Raman enhancement of ^{Z}diP on the Ag electrode.[39] In turn, the presence of the asymmetric stretching vibration of the COO^- group along with $\nu_s(COO^-)$ (1354 cm^{-1}) would indicate a monodentate orientation of this moiety through one oxygen atom, as suggested by Castro and co-workers in SERS studies on α-phenylglycine.[40] Undoubtedly, the interaction of the carboxylate moiety with the silver electrode is strong because the $\nu_s(COO^-)$ mode is red-shifted by ca. 30 cm^{-1} in comparison to the position of this band in the Raman spectrum of the solution.

Gly-$\Delta^{(E)}$Phe (^{E}diP). The careful inspection of Figure 4B and Table 2 reveals several features of interest for the SERS of the dipeptide containing the *E* isomer of ΔPhe. In contrast to the spectra of ^{Z}diP, the SERS spectra of ^{E}diP on the silver colloid show differences in the pH ranges of 2−5 and 7−9 (cf. Figure 4B). Nevertheless, both sets of the bands appear at almost the

dx.doi.org/10.1021/jp500650p | J. Phys. Chem. B XXXX, XXX, XXX−XXX

Table 1. Selected IR, Raman, and SERS Bands (cm^{-1}) of Gly-$\Delta^{(Z)}$Phe in the Region 400−1800 cm^{-1} and Their Tentative Assignments (%, PED >10% Shown) Based on Calculations[a]

		SERS colloid		SERS electrode	
FT-IR	FT-NR solid	pH 2.0−7.0	pH 9.0	pH 2.0−9.0	assignment
1706vs	1705w				72 amide I
1655m	1647vs	1647vs	1647m	1643m	51 $\nu(C_\alpha{=}C_\beta)$, 20 amide I
1626m	1626w,sh	1619m	1618vs		93 $\delta_{as}(NH_3^+)$
	1599s	1599vs	1597vs	1598vs	82 ^{Ph}8a
	1576w	1579w			
				1574vs,sh	$\nu_{as}(COO^-)$ or 8b
1537vs			1537w	1527m,sh	63 amide II
1508vs					
1493vs	1493vw	1493w	1493m		34 $\delta(CH_2)$, 29 $\delta_s(NH_3^+)/\delta(NH_2)$, 15 amide II
1450w	1447w	1449w			45 $\delta(CH_2)$, 42 $\delta_s(NH_3^+)$
1427w		1426w	1425s		76 ^{Ph}19b
1382vs	1383m[b]	1368m,br	1365vs,br	1354m,br	86 $\nu_s(COO^-)$
	1295vw	1296w	1298m		70 $\tau(CH_2)$
	1282vw	1280vw	1282m		69 ^{Ph}3
1211w	1209s	1212s	1217s	1211m	75 ^{Ph}13
	1190w	1186m	1185vs	1185w	89 ^{Ph}9a
	1159w	1162w	1162s		90 ^{Ph}9b
1080w			1077w	1072w	60 $\rho(NH_3^+)$
	1032w	1032w	1031m	1031w	76 ^{Ph}18a
	1001s	1003s	1002m	1002m	76 ^{Ph}12
920w	923vw		919m		53 $\rho(CH_2)$, 23 $\rho(NH_3^+)$, 15 ω(C=O)
790w		800w	800s		71 $\delta(COO^-)$
733s			734m		35 $\delta(COO^-)$, 13 ν(CC)
532s	533w	529w		543m	32 $\tau(COO^-)$
		441w	440vs		50 ^{Ph}16b
403m	403w	403w		406m	86 ^{Ph}16a

[a]B3LYP/6-311++G(d,p). Key: ν, stretching; δ, scissoring; ρ, rocking; ω, wagging; τ, twisting; s, symmetric; as, asymmetric; vs, very strong; s, strong; m, medium; w, weak; vw, very weak; sh, shoulder. [b]In the spectrum of 0.1 M solution at pH of 5.0−9.0.

same wavenumbers, indicating that the same functional groups interact with the Ag nanoparticles, but with a different contribution. A band at 1392 cm^{-1} [$\nu_s(COO^-)$] is slightly blue-shifted from the position in the normal Raman spectrum of the solid (3−4 cm^{-1}), suggesting that the electronic structure of the group is not strongly disturbed upon the adsorption on the metal and its orientation is planar because the scissoring mode of the deprotonated carboxylic group around 800 cm^{-1} exhibits low intensity compared to that of the $\nu_s(COO^-)$ mode. The absence of vibrational modes of the NH_2/NH_3^+ groups for the *E* isomer points out participation of only the C- terminus in interactions with the metal, whereas both the terminal groups were involved in adsorption for the ^{Z}diP.

The SERS enhancement of the 1636 cm^{-1} band [$\nu(C_\alpha{=}C_\beta)$] is significant in the entire pH range, in contrast to the *Z* isomer. The difference is the most visible when SERS spectra collected for ^{Z}diP and ^{E}diP under alkaline pH are compared (Figure 3B and 4B, respectively). This spectral feature may indicate a strong overlap of π orbitals of the C=C moiety with metal orbitals for *E* isomer, resulting in amplification of the band corresponding to the $\nu(C_\alpha{=}C_\beta)$ vibration. On the other hand, a band at 1002 cm^{-1} (12) is the most enhanced SERS band among the phenyl ring modes for ^{E}diP in contrast to ^{Z}diP for which the 8a vibration was the most amplified. The observed difference between the two isomers of dipeptide suggests a more tilted orientation of the phenyl ring for ^{E}diP adsorbed on the Ag colloid than for ^{Z}diP.

Similarly to the *Z* isomer of the dipeptides, the interaction of ^{E}diP with the silver electrode gives the same spectral motif in the full range of pH. An examination of the SERS spectrum in Figure 4B shows a very high enhancement of a band at 1345 cm^{-1} attributed to the $\nu_s(COO^-)$ mode. The position of this band shifts down in comparison to the SERS spectrum for the Ag colloid in the acidic solution by ca. 50 cm^{-1}, indicating very strong chemisorption of this group. In contrast to SERS on the colloidal particles, the intensity of the 1630 cm^{-1} band [$\nu(C_\alpha{=}C_\beta)$] decreases in favor of the 8a and 8b/$\nu_{as}(COO^-)$ modes that are observed at 1599 and 1578 cm^{-1}, respectively, as in the case of ^{Z}diP (cf. Tables 1 and 2). Moreover, this interaction leads to medium enhancement of the bands originating from the amide II (1543 cm^{-1}) and the rocking vibration of the =CH group (1458 cm^{-1}). At first glance, this SERS spectrum is similar to the SERS spectrum of ^{Z}diP on the Ag electrode and a difference mainly concerns relative intensity of the $\nu_s(COO^-)$ mode. It suggests that due to the lack of steric hindrance in ^{E}diP, the carboxylate group of this molecule can easily participate in the interactions with the metal.

Gly-$\Delta^{(Z)}$Phe-Gly (^{Z}triP). SERS spectra of Gly-$\Delta^{(Z)}$Phe-Gly (^{Z}triP) are shown in Figure 5B and the assignment of the observed vibrational bands is collected in Table 3. ^{Z}triP is the only peptide studied here that shows distinct spectral profile in acidic, neutral, and alkaline environments upon the adsorption on the silver nanocolloidal particles (cf. Figure 5B). All SERS spectra show the presence of strong and broad bands of the $\nu_s(COO^-)$ mode in the range 1370−1380 cm^{-1} that are shifted from 1398 cm^{-1} in the normal Raman spectrum (Figure 5A). As observed for the previous peptides, deprotonation of the carboxylic group appears due to the adsorption on the Ag

dx.doi.org/10.1021/jp500650p | J. Phys. Chem. B XXXX, XXX, XXX−XXX

Table 2. Selected IR, Raman, and SERS Bands (cm^{-1}) of Gly-$\Delta^{(E)}$Phe in the Range 500−1700 cm^{-1} and Their Tentative Assignments (%, PED >10% Shown) Based on Calculations[a]

		SERS colloid		SERS electrode	
FT-IR	FT-NR solid	pH 2.0−5.0	pH 7.0−9.0	pH 2.0−9.0	assignment
1687m	1682vw				72 amide I
1632m	1634vs	1636vs	1636vs	1630s	61 $\nu(C_\alpha{=}C_\beta)$
1595m	1601vs	1599m	1599m	1599vs	74 ^{Ph}8a
	1574w	1579w	1576w		
				1578s	$\nu_{as}(COO^-)$ or 8b
1548vs				1543s	62 amide II
1431s	1430w			1458m	37 ρ(=CH), 13 ν(CC)
1388m		1392s,br	1391m,br	1345vs,br	65 $\nu_s(COO^-)$
1287s	1287m	1288m	1288m		71 $\tau(CH_2)$
1260s,sh				1251m	32 ^{Ph}3, 22 $\nu_s(COO^-)$
1218w	1219m	1217m	1220m		72 ^{Ph}13
	1179m	1185m	1183m		91 ^{Ph}9a
1159m	1160w,sh	1162w,sh		1156w	88 ^{Ph}9b
1076w				1086w	55 $\rho(NH_3^+)$, 13 $\omega(CH_2)$
1028w	1030w	1031m	1032w		76 ^{Ph}18a
	1001s	1002vs	1002m	1000m	84 ^{Ph}12
962m	961w	948m,br	953w,br		42 β(CNC), 11 ρ(C=O), 10 ν(CC)
928s			927w,br		52 $\rho(CH_2)$, 24 $\rho(NH_3^+)$, 15 ω(C=O)
837m		837m	838w		46 $\omega(COO^-)$, 11 ν(CC)
	814w	797m			64 $\delta(COO^-)$, 16 ω(CNC)
	677w	678w	675w		75 ^{Ph}5
				542m	38 $\tau(COO^-)$[b]

[a]B3LYP/6-311++G(d,p). Key: ν, stretching; δ, scissoring; ρ, rocking; ω, wagging; β, in-plane bending; τ, twisting; s, symmetric; as, asymmetric; vs, very strong; s, strong; m, medium; w, weak; vw, very weak; sh, shoulder. [b]According to the theoretical spectrum.

Table 3. Selected IR, Raman, and SERS Bands (cm^{-1}) of Gly-$\Delta^{(Z)}$Phe-Gly in the Range 400−1700 cm^{-1} and Their Tentative Assignments (%, PED >10% Shown) Based on Calculations[a]

		SERS colloid			SERS electrode	
FT-IR	FT-NR solid	pH 2.0	pH 5.0−7.0	pH 9.0	pH 2.0−9.0	assignment
1697m	1701m					amide I (out-of-phase)
1657m	1659s		1656w,sh	1656w,sh		amide I (in-phase)
1615s	1615vs	1622vs	1618vs	1618s		67 $\nu(C_\alpha{=}C_\beta)$
1596w,sh	1599s	1598w	1602s	1602s	1597s	77 ^{Ph}8a
	1576m		1574w	1574w		$\nu_{as}(COO^-)$ or 87 ^{Ph}8b
1540m,sh	1532w,br					69 amide II
1511vs						70 amide II
1494m,sh	1493w	1495w	1495w	1493m		56 $\delta_s(NH_3^+)/\delta(NH_2)$
	1428vw	1429m				57 ^{Ph}19b
1398vs	1398w	1370s,br	1380vs,br	1375s,br		88 $\nu_s(COO^-)$
1306m		1301m		1299s,br		32 $\omega(CH_2)$
	1292w	1286m				68 $\tau(CH_2)$
	1205vs	1222s	1215s	1215m		73 ^{Ph}13
	1187m	1187s	1188m	1189w		91 ^{Ph}9a
1153vw	1157w	1164s				90 ^{Ph}9b
	1035m	1032w	1035m	1032w		77 ^{Ph}18a
	1000s	1005m	1004vs	1004vs	1001s	71 ^{Ph}12
957m	959m		955s,br	955s,sh		35 β(CNC), 15 ν(CN)
925m,sh		921m	924s,br	930s,br		27 ν(CC), 18 ν(CN)
840m	840w		840w			59 ν(CC), 21 $\omega(COO^-)$
		803s	814w			47$\delta(COO^-)$
551m					552s,br	41 $\tau(COO^-)$
		443s				62 ^{Ph}16b[b]

[a]B3LYP/6-311++G(d,p). Key: ν, stretching; δ, scissoring; ρ, rocking; ω, wagging; β, in-plane bending; τ, twisting; s, symmetric; as, asymmetric; vs, very strong; s, strong; m, medium; w, weak; vw, very weak; sh, shoulder. [b]According to the theoretical spectrum.

surface, and next due to their interaction through chemisorption. The scissoring mode of the COO^- group appears as a strong band at 803 cm^{-1} for pH 2 only, which indicates a tilted orientation of the carboxylate group adsorbed on the surface

dx.doi.org/10.1021/jp500650p | J. Phys. Chem. B XXXX, XXX, XXX−XXX

Table 4. Selected IR, Raman, and SERS Bands (cm^{-1}) of Gly-$\Delta^{(E)}$Phe-Gly in the Range 400−1700 cm^{-1} and Their Tentative Assignments (%, PED >10% Shown) Based on Calculations[a]

		SERS colloid		SERS electrode	
FT-IR	FT-NR solid	pH 5.0−7.0	pH 9.0	pH 2.0−9.0	assignment
1664m	1651s,sh				amide I (out-of-phase)
1632m	1632vs		1635vs, sh		amide I (in-phase)
	1620s	1623vs	1624vs		53 $\nu(C_\alpha{=}C_\beta)$
1606m	1603vs	1602m	1604vs	1601vs	82 ^{Ph}8a
	1576w		1574w		59 ^{Ph}8b, 29 $\nu_{as}(COO^-)$
1541m					67 amide II
1507vs					57 amide II
1499vs	1498w	1496m	1496w	1498s	65 $\delta_s(NH_3^+)/\delta(NH_2)$, 10 $\delta(CH_2)$
	1412vw	1429m			80 $\delta(CH_2)$
1391s		1370s,br	1383m,br	1349s,br	81 $\nu_s(COO^-)$
1304m	1304w	1301m	1301m		45 $\omega(CH_2)$
	1292w	1287m			68 $\tau(CH_2)$
	1221m	1222m	1222m		45 ^{Ph}13
1186w	1182m	1188s	1188m		87 ^{Ph}9a
1159w	1159vw	1165s	1163m		88 ^{Ph}9b
1073vw		1079m			52 $\rho(NH_3^+)$, 18 $\omega(CH_2)$
1033m	1034w	1033m	1033m		74 ^{Ph}18a
	1003m	1005s	1005s	1003s	77 ^{Ph}12
925m		922m	934m,br		52 $\rho(CH_2)$, 18 $\rho(NH_3^+)$
918m	917vw				80 17b
874m	876m		884w		50 $\rho(=CH)$, 16 $\tau(C{=}C)$
843m	843w	838m	843w		47 $\nu(CC)$, 28 $\omega(COO^-)$
	802w	804vs	803m		60 $\delta(COO^-)$
	465vw	444vs			56 ^{Ph}16b

[a]B3LYP/6-311++G(d,p). Key: ν, stretching; δ, scissoring; ρ, rocking; ω, wagging; β, in-plane bending; τ, twisting; s, symmetric; as, asymmetric; vs, very strong; s, strong; m, medium; w, weak; vw, very weak; sh, shoulder.

through both oxygen atoms.[36,37] Then, after increasing pH, the ^{Z}triP molecules adopt a more flat geometry, corresponding to adsorption through π-electrons, because $\nu_s(COO^-)$ is considerably stronger than a band of the $\delta(COO^-)$ vibration. One of the most intense bands in all SERS spectra on the Ag colloid is a band observed at ca. 1620 cm^{-1} [$\nu(C_\alpha{=}C_\beta)$]. In turn, a shoulder at 1656 cm^{-1} in the SERS spectra recorded at pH above 5.0 originates from the in-phase amide I vibration.

Following variations in intensity of the ring modes at ca. 1600 (8a) and 1005 cm^{-1} (12), one can see that both vibrations are less enhanced at pH 2, and their intensities increase significantly with respect to the $\nu(C_\alpha{=}C_\beta)$ mode (at 1620 cm^{-1}) upon a pH increase. In turn, several ring modes appear at 1429 (19b), 1222 (13), 1187 (9a), 1164 (9b), and 443 (16b) cm^{-1} in the SERS spectrum recorded in the acidic environment, and they are attributed to the in- as well as out-of-plane vibrations of the phenyl ring (see Table 3 for detail). Moreover, the significant enhancement is observed for the out-of-plane ring bend of the ring at ca. 440 cm^{-1} at pH 2. Furthermore, the presence of medium-intensity bands at 1301 and 1286 cm^{-1}, originating from the bending vibrations of the CH_2 group, indicates that the glycine residues are present in close proximity to the metal at low pH. At pH between 5 and 9, the SERS signal is observed for the in-plane bending vibrations at 1215 (13), 1188 (9a), and 1035 cm^{-1} (18a) along with the strong intensification of the 8a and 12 modes. These features suggest a change in the phenyl ring orientation from tilted to more flat, accompanied by a change in the orientation of the carboxylate group. Then due to pH increasing to 9, SERS intensification of $\delta(NH_3^+)/\delta(NH_2)$ at 1493 cm^{-1} and $\omega(CH_2)$ at 1299 cm^{-1} along with the skeletal modes at 924 and 955 cm^{-1} suggests additional interactions of the *Z* tripeptides with the silver via the CC skeleton and amino moieties.

The SERS spectrum recorded by the use of the electrode substrate shows the presence of three bands only (cf. Figure 5B). Two of them originate from modes of the phenyl ring, i.e., at 1001 (12) and 1597 cm^{-1} (8a) that are usually observed in SERS. A minor shift and broadening of these bands indicate that the long-distance electromagnetic mechanism predominates in SERS enhancement.

Gly-$\Delta^{(E)}$Phe-Gly (^{E}triP). Raman and SERS spectra of the tripeptide containing the $\Delta^{(E)}$Phe isomer (^{E}triP) are shown in Figure 6. Table 4 collects positions of Raman and SERS bands with their tentative assignments. SERS signal was not observed for the solution at pH 2, whereas distinct SERS profiles were found for the weakly acidic/neutral and alkaline environment. Interestingly, the SERS spectrum of ^{E}triP at pH of 5−7 is very similar to the SERS spectrum of ^{Z}triP but at a pH of 2 (cf. Figures 5B and 6B). Enhancement of Raman bands considerably changes after increasing pH (Figure 6B). First of all, the $\nu_s(COO^-)$ vibration loses its intensity and its wavenumber slightly changes (two components around 1370 and 1380 cm^{-1} at pH 5−7, but only one at 1383 cm^{-1} at pH 9), suggesting that the interaction of this group with the metal is weaker than for ^{Z}triP. At a pH of 5−7 this band is accompanied by a relatively strong scissoring mode of the carboxylate ion at 804 cm^{-1}, indicating a tilted orientation of the COO^- group through both oxygen atoms on the Ag surface, and then becoming more flat at a pH of 9. The most prominent bands in SERS spectra on the Ag colloid are observed in the region 1600−1640 and at 1005 cm^{-1}, and they are assigned to the $\nu(C_\alpha{=}C_\beta)$, in-phase amide I (only pH 9), 8a, and 12

dx.doi.org/10.1021/jp500650p | J. Phys. Chem. B XXXX, XXX, XXX−XXX

vibrations, respectively. They are sharp and have only minor shifts compared to the normal Raman spectrum of ^{E}triP. This indicates that the dehydro residue is oriented almost perpendicularly with the same orientation of the amide bonds at the alkaline solution. The other modes of the phenyl ring originating from its in-plane motions are found in the region 1060−1230 cm^{-1}, confirming this hypothesis.

In turn, a few SERS bands are observed after adsorption of ^{E}triP on the silver electrode. Sharp bands at 1003/1601 and 1498 cm^{-1} assigned to the 12/8a modes and $\delta_s(NH_3^+/NH_2)$ vibrations indicate the participation of the phenyl and amino groups in interactions with the metal. The presence of a broad, strong-intensity band at 1349 cm^{-1} is similar to the band found in SERS on the Ag electrode of ^{E}diP. Their broadening and significant red shift compared to the counterparts in the SERS spectra on the Ag sol and in the normal Raman spectrum can be considered as a marker band of the *E* dehydropeptide−electrode interactions. The molecules adsorb in a flat orientation of the carboxylate, which is supported by the absence of the bending and asymmetric stretching modes of the COO^- group.

4. CONCLUSIONS

Surface-enhanced Raman spectroscopy revealed interesting facts on the interaction of the di- and tridehydropeptides containing both isomers of the ΔPhe residue with Ag colloidal particles and bulk, nanostructured electrode. The adsorption mode of the molecules studied here is very sensitive to the type of isomer, the elongation of the backbone, and the SERS-active substrate preparation method and chemical surroundings of the molecule. Anyhow, the SERS activity of the dehydropeptides studied here is more informative for molecules adsorbed on the silver colloidal nanoparticles than on the electrode.

First, a substantial shift and broadening of the symmetric stretching vibrations of the carboxylate groups was observed in the SERS spectra recorded on both the silver substrates. We propose that this group adopts a flat or slightly tilted orientation on the metal surface. The enhancement of this mode is different for each adsorbate, and thus it is not straightforward to correlate it with the molecular structure and/or acidity of the solution. Only for the *E* dehydropeptides did we observed decreasing SERS intensity of this mode in the alkaline solution. However, the respective population of the neutral/anionic/cationic forms of the molecules may vary due to the adsorption on the silver surface, because the metal surface can change the p*K* of the analyte. In turn, the adsorption on the silver electrode leads to a greater disturbance of the π-electron system of the COO^- group than on the silver sol, resulting simply from the positive-charged surface of the electrode at open circuit potential.

The presence of the >C═CH—Ph moiety also affects the adsorption profile of the peptides. The relative enhancement of the phenyl and C_α═C_β modes changes. The alternation in the SERS intensity of the C_α═C_β stretching mode due to the interaction with both silver substrates indicates that the orientation of this group on the metal is enforced by the orientation of the surrounding moieties unlike for the Boc-Gly-ΔPhe peptides studied previously in that these were oriented perpendicularly to the Ag nanoparticles.[20] In turn, the phenyl ring adopts various orientations that are correlated with the enhancement of its modes. However, most SERS spectra for the $\Delta^{(Z)}$Phe peptides exhibit a stronger enhancement of vibrations of the phenyl ring than the *E* counterparts. Furthermore, some SERS spectra are dominated by signals coming from the N-terminal groups, indicating their participation in the interaction with the metal, especially for the silver colloid. Interestingly, their enhancement is stronger for the *Z* isomers than the *E* peptides, similarly to their coordination fashion toward transition metal ions.

■ ASSOCIATED CONTENT

Ⓢ Supporting Information

Internal coordinates used in calculation of PED of the theoretical modes of di- and tridehydropeptides (Table S1). Comparison of experimental (solid) and computed IR and Raman spectra of ^{Z}diP (Figure 1S). Comparison of experimental (solid) and computed IR and Raman spectra of ^{E}diP (Figure 2S). Comparison of experimental (solid) and computed IR and Raman spectra of ^{Z}triP (Figure 3S). Comparison of experimental (solid) and computed IR and Raman spectra of ^{E}triP (Figure 4S). This information is available free of charge via the Internet at http://pubs.acs.org

■ AUTHOR INFORMATION

Corresponding Author

*K. Malek: e-mail, malek@chemia.uj.edu.pl; tel, +48 12 663 2064; fax, +48 12 634 0515.

Author Contributions

The manuscript was written through contributions of all authors. All authors have given approval to the final version of the manuscript.

Notes

The authors declare no competing financial interest.

■ ACKNOWLEDGMENTS

K.M. thanks the Polish Ministry of Science and Higher Education for the financial support (grant No. N N204 333037 in 2009-2011). Calculations were done at the Academic Computer Center "Cyfronet", Krakow, Poland (Grant MNiI/SGI2800/UJ/003/2005), which is acknowledged for computing time.

■ REFERENCES

(1) Schlücker, S. Surface Enhanced Raman Spectroscopy. *Analytical, Biophysical and Life Science Applications*; Wiley-VCH: Weinheim, Germany, 2011.

(2) Castro, J. L.; Lopez-Raminez, M. R.; Lopez Tocon, I.; Otero, J. C. Vibrational Study of the Metal−Adsorbate Interaction of Phenylacetic Acid and α-phenylglycine on Silver Surfaces. *J. Colloid Interface Sci.* **2003**, *263*, 357−363.

(3) Wie, F.; Zhang, D.; Halas, N. J.; Hartgerink, J. D. Aromatic Amino Acids Providing Characteristic Motifs in the Raman and SERS Spectroscopy of Peptides. *J. Phys. Chem. B* **2008**, *112*, 9158−9164.

(4) Larsson, M.; Lindgren, J. Analysis of Glutathione and Immunoglobulin G Inside Chromatographic Beads Using Surface-Enhanced Raman Scattering Spectroscopy. *J. Raman Spectrosc.* **2005**, *36*, 394−399.

(5) Krolikowska, A.; Bukowska, J. Surface-Enhanced Resonance Raman Spectroscopic Characterization of Cytochrome c Immobilized on 2-mercaptoethanesulfonate Monolayers on Silver. *J. Raman Spectrosc.* **2010**, *41*, 1621−1631.

(6) Huang, H.; Xie, J.; Liu, X. L.; Yuan, L.; Wang, S. S.; Guo, S. X.; Yu, H. R.; Chen, H.; Zhang, Y. L.; Wu, X. H. Conformational Changes of Protein Adsorbed on Tailored Flat Substrates with Different Chemistries. *Chem. Phys. Chem.* **2011**, *12*, 3642−3646.

(7) Garrido, C.; Aliaga, A. E.; Gomez-Jeria, J. S.; Clavijo, R. E.; Campos-Vallette, M. M.; Sanchez-Cortes, S. Adsorption of Oligopep-

tides on Silver Nanoparticles: Surface-Enhanced Raman Scattering and Theoretical Studies. *J. Raman Spectrosc.* **2010**, *41*, 1149−1155.
(8) Gupta, A.; Mehrotra, R.; Klimov, E.; Siesler, H. W.; Joshi, R. M.; Chauhan, V. S. Thermal Stability of Dehydrophenylalanine-Containing Model Peptides as Probed by Infrared Spectroscopy: A Case Study of an α-Helical and a 3_{10}-Helical Peptide. *Chem. Biodiver.* **2006**, *3*, 284−295.
(9) Kotha, S. The Building Block Approach to Unusual α-Amino Acid Derivatives and Peptides. *Acc. Chem. Res.* **2003**, *36*, 342−351.
(10) Chatterjee, C.; Paul, M.; Xie, L.; Van Der Donk, W. A. Biosynthesis and Mode of Action of Lantibiotics. *Chem. Rev.* **2005**, *105*, 633−684.
(11) Yamada, K.; Shinoda, S.; Oku, H.; Komagoe, K.; Katsu, T.; Katakai, R. Synthesis of Low-Hemolytic Antimicrobial Dehydropeptides Based on GramicidinS. *J. Med. Chem.* **2006**, *49*, 7592−7595.
(12) Barsby, T.; Warabi, K.; Sørensen, D.; Zimmerman, W. T.; Kelly, M. T.; Andersen, R. J. The Bogorol Family of Antibiotics: Template-Based Structure Elucidation and a New Approach to Positioning Enantiomeric Pairs of Amino Acids. *J. Org. Chem.* **2006**, *71*, 6031−6037.
(13) Świątek-Kozłowska, J.; Brasuń, J.; Chruściński, L.; Chruścińska, E.; Makowski, M.; Kozłowski, H. Impact of α,β-dehydroamino Acid Residues on the Binding Abilities of Di-, Tri- and Tetra-Peptides. *New J. Chem.* **2000**, *24*, 893−896.
(14) Świątek-Kozłowska, J.; Brasuń, J.; Łuczkowski, M.; Makowski, M. Binding Abilities of Dehydropeptides Towards Cu(II) and Ni(II) Ions. Impact of Z-E Isomerization on Metal Ion Binding. *J. Inorg. Biochem.* **2002**, *90*, 106−112.
(15) Demizu, Y.; Yamagata, N.; Sato, Y.; Doi, M.; Tanaka, M.; Okuda, H.; Kurihara, M. Controlling the Helical Screw Sense of Peptides with C-terminal L-valine. *J. Pept. Sci.* **2010**, *16*, 153−158.
(16) Komori, H.; Inai, Y. Electronic CD Study of a Helical Peptide Incorporating Z-Dehydrophenylalanine Residues: Conformation Dependence of the Simulated CD Spectra. *J. Phys. Chem. A* **2006**, *110*, 9099−9107.
(17) Makowski, M.; Lisowski, M.; Mikolajczyk, I.; Lis, T. N-[tert-Butoxycarbonylglycyl-(E)-α,β-dehydrophenylalanylglycylglycyl-(E)-α,β-dehydrophenylalanyl]glycine. *Acta Cryst. E* **2007**, *63*, o19−o21.
(18) Broda, M. A.; Buczek, A.; Siodlak, D.; Rzeszotarska, B. The Effect of β-Methylation on the Conformation of α,β-Dehydrophenylalanine. *J. Pep. Sci.* **2009**, *15*, 465−473.
(19) Siodlak, D.; Broda, M. A.; Rzeszotarska, B. Conformational Analysis of α,β-Dehydropeptide Models at the HF and DFT Levels. *J. Mol. Structr. (Teochem)* **2004**, *668*, 75−85.
(20) Malek, K.; Makowski, M.; Królikowska, A.; Bukowska, J. Comparative Studies on IR, Raman, and Surface Enhanced Raman Scattering Spectroscopy of Dipeptides Containing ΔAla and ΔPhe. *J. Phys. Chem. B* **2012**, *116*, 1414−1425.
(21) Malek, K.; Makowski, M. The Infrared and Raman Spectra of Solid Tridehydropeptides: Influence of ΔAla and ΔPhe on the Spectral Profile. *Vib. Spectrosc.* **2012**, *60*, 73−78.
(22) Makowski, M.; Rzeszotarska, B.; Smelka, L.; Kubica, Z. Synthesis of Peptides with α,β-Dehydroamino Acids, III. Debenzyloxycarbonylation and Detrifluoroacetylation of Dehydroalanine and Dehydrophenylalanine Peptides. *Liebigs Ann.Chem.* **1985**, 1457−1464.
(23) Lee, P. C.; Meisel, D. Adsorption and Surface-Enhanced Raman of Dyes on Silver and Gold Sols. *J. Phys. Chem.* **1982**, *86*, 3391−3395.
(24) Frisch, M. J.; Trucks, G. W.; Schlegel, H. B.; Scuseria, G. E.; Robb, M. A.; Cheeseman, J. R.; Montgomery, Jr., J. A.; Vreven, T.; Kudin, K. N.; Burant, J. C.; et al. Gaussian 09, Revision A. 1; Gaussian, Inc.: Wallingford, CT, 2009.
(25) Becke, A. D. Density-Functional Thermochemistry. III. The Role of Exact Exchange. *J. Chem. Phys.* **1993**, *98*, 5648−5652.
(26) Lee, C.; Yang, W.; Parr, R. G. Development of the Colle-Salvetti Conelation Energy Formula into a Functional of the Electron Density. *Phys. Rev. B: Condens. Matter Mater. Phys.* **1988**, *37*, 785−789.
(27) Caricato, M.; Mennucci, B.; Tomasi, J.; Ingrosso, F.; Cammi, R.; Corni, S.; Scalmani, G. Formation and Relaxation of Excited States in Solution: A New Time Dependent Polarizable Continuum Model Based on Time Dependent Density Functional Theory. *J. Chem. Phys.* **2006**, *124*, 124520−124513.
(28) Chowdhry, B. Z.; Dines, T. J.; Jabeen, S.; Withnall, R. Vibrational Spectra of α-Amino Acids in the Zwitterionic State in Aqueous Solution and the Solid State: DFT Calculations and the Influence of Hydrogen Bonding. *J. Phys. Chem. A* **2008**, *112*, 10333−10347.
(29) Budesınsky, M.; Danecek, P.; Bednarova, L.; Kapitan, J.; Baumruk, V.; Bour, P. Comparison of Quantitative Conformer Analyses by Nuclear Magnetic Resonance and Raman Optical Activity Spectra for Model Dipeptides. *J. Phys. Chem. A* **2008**, *112*, 8633−8640.
(30) Michalska, D.; Wysokinski, R. The Prediction of Raman Spectra of Platinum(II) Anticancer Drugs by Density Functional Theory. *Chem. Phys. Lett.* **2005**, *403*, 211−217.
(31) Marzec, K. M.; Gawel, B.; Lasocha, W.; Proniewicz, L. M.; Malek, K. Interaction Between Rhodanine and Silver species on a Nanocolloidal Surface and in the Solid State. *J. Raman Spectrosc.* **2009**, *41*, 543−552.
(32) Marzec, K. M.; Reva, I.; Fausto, R.; Malek, K.; Proniewicz, L. M. Conformational Space and Photochemistry of α-Terpinene. *J. Phys. Chem. A* **2010**, *114*, 5526−5536.
(33) Pulay, P.; Fogarasi, G.; Pang, F.; Boggs, J. E. Systematic Ab Initio Gradient Calculation of Molecular Geometries, Force Constants and Dipole-moment Derivatives. *J. Am. Chem. Soc.* **1979**, *101*, 2550−2560.
(34) Fogarasi, G.; Zhou, X.; Taylor, P. W.; Pulay, P. The Calculation of Ab Initio Molecular Geometries: Efficient Optimization by Natural Internal Coordinates and Empirical Correction by Offset Forces. *J. Am. Chem. Soc.* **1992**, *114*, 8191−8201.
(35) Martin, J. M. L.; Van Alsenoy, C. *Gar2ped*; University of Antwerp, 1995.
(36) Gupta, A.; Chauhan, V. S. Synthetic and Conformational Studies on Dehydroalanine-Containing Model Peptides. *Biopolymers* **1990**, *30*, 395−403.
(37) Suh, J. S.; Moskovits, M. Surface-enhanced Raman Spectroscopy of Amino Acids and Nucleotide Bases Adsorbed on Silver. *J. Am. Chem. Soc.* **1986**, *108*, 4711−4718.
(38) Suh, J. S.; Kim, J. Three Distinct Geometries of Surface-Adsorbed Carboxylate Groups. *J. Raman Spectrosc.* **1998**, *29*, 143−148.
(39) Fleger, Y.; Mastai, Y.; Rosenbluh, M.; Dressler, D. H. SERS as a Probe for Adsorbate Orientation on Silver Nanoclusters. *J. Raman Spectrosc.* **2009**, *40*, 1572−1577.
(40) Castro, J. L.; Lopez-Raminez, M. R.; Lopez Tocon, I.; Otero, J. C. Vibrational Study of the Metal−Adsorbate Interaction of Phenylacetic Acid and α-Phenylglycine on Silver Surfaces. *J. Colloid Interface Sci.* **2003**, *263*, 357−363.